

## **Three Dimensional Artifact Free Visualization of Different Metallic Intervertebral Disc Spacers With Flat Panel Detector Volume CT (FD-VCT): A Comparative Cadaveric Spine Study**

**Prof. Dr. Thorsten Ernstberger**

Clinic of Spinal Surgery  
Klinikum Bad Bramstedt  
Oskar-Alexander-Strasse 26, 24576 Bad Bramstedt  
Germany

**Christian Dullin, D.Sc.**

Department of Diagnostic Radiology  
University of Göttingen  
Robert-Koch-Strasse 40, 37099 Göttingen  
Germany

**Gottfried Buchhorn, M.Eng.**

Biomaterial Laboratory  
Department of Orthopedic Surgery  
University of Göttingen, Robert-Koch-Strasse 40, 37099 Göttingen  
Germany

**Gabert Heidrich, M.D.**

Center of Radiology Weilheim  
Ambulatory Healthcare Center  
Röntgenstrasse 2-4, 82362 Weilheim i. Obb  
Germany

### **Abstract**

*Image quality and implant detectability by conventional imaging methods are suboptimal for perioperative spinal diagnostics, primarily limited by implant-related artifacts. This preclinical experimental study aimed to evaluate the imaging quality of two different metallic intervertebral spacers used as stand alone cages examined by flat-panel detector-based volumetric computed tomography (FD-VCT) versus MRI. Both spacer types (titanium, cobalt-chrome-molybdenum) were implanted in a porcine cadaver spine and then examined by MRI using T1-weighted turbo spin echo sequences. Comparative imaging was performed with an experimentally approved FD-VCT prototype featuring 2D and 3D imaging and high isotropic spatial resolution. Data analysis focused on spacer shape, implant positioning and implant-bone interface. Compared to MRI, image quality and detectability of all target characteristics were better with FD-VCT and without the usual artifacts. Using its option for implant-specific imaging, the experimental FD-VCT imager allowed reliable determination of additional data such as dimension and volume. These experiments provide initial evidence that FD-VCT produces an excellently artifact-free imaging considering distinguishing key characteristics of intervertebral implants. Thus, FD-VCT appears to be the ideal modality in preclinical studies for evaluation of osseous integration processes secondary to interbody spondylodesis.*

**Key Words:** Metallic intervertebral disc spacers, flat panel detector based volumetric CT, magnetic resonance imaging (MRI), artifacts, implant imaging

### **Introduction**

Magnetic resonance imaging (MRI) are established radiological methods used in spinal diagnostics.

These procedure, however, can be fraught with the limitations of suboptimal image quality caused by surgically implanted foreign material [1]. In the majority of degenerative spinal diseases, interbody cages and spacers are implanted to bridge intervertebral spaces. In our department, MRI is the radiological diagnostic method of choice for clarifying post-fusion questions regarding the involvement of osseous and soft tissue structures in relation to implant position. In these indications, MRI is better suited than multisection CT to demonstrate myelopathies, inflammatory and infectious processes and neurodegenerative changes.

This preclinical experimental study aimed to evaluate the imaging quality of 2 different metallic intervertebral spacers implanted in a cadaveric porcine spine scanned by flat panel detector-based volume computed tomography (FD-VCT) using a prototype high-resolution imager approved for experimental applications [2]. FD-VCT is a newly emerging technology in radiology that can produce both 2-dimensional and 3-dimensional images as well as volumetric measurements. Thanks to its high local resolution, FD-VCT systems are capable of detecting interpolation structures in high-contrast range .

The findings obtained by FD-VCT were compared with identical scans of the spacers taken by magnetic resonance imaging (MRI). This analysis mainly focused on the potential for FD-VCT to better distinguish the target characteristics of implant position, implant shape and implant-bone interface. Our hypothesis was that an artifact-free and detailed assessment of the implanted intervertebral spacers would be possible with regard to the targeted characteristics.

## **Methods**

### **Experimental porcine model**

The spinal column of a domestic pig that had been slaughtered for human consumption was used for our experimental cadaveric model. The animal originated from a slaughterhouse that was subject to regular veterinary inspection and monitoring. The entire spinal column was completely dissected and removed with the surrounding skin and paravertebral muscles attached for subsequent diagnostic imaging analysis. On the ventral side, the lumbar spine was kept covered by the psoas muscles bilaterally. Particular care was taken to preserve all intraspinal and extraspinal neural structures. According to the experimental protocol, the caudal third of the thoracic spine and the entire lumbar spine had to be retained.

A preliminary examination was conducted so that we could estimate the effects of artifacting with the greatest accuracy: The cobalt-chrome spacers were incorporated in a homogeneous mass of ground pork meat and MRI test measurements were carried out on this simulated model. The test simulation with various MRI sequences allowed us to determine that the maximum artifact width for the metal spacers was 6.5 cm. This artifact width defined the minimum distance for implantation of the intervertebral spacers and for cortical bone grafting. The MRI trial run showed that it was necessary to provide soft tissue mass around the cadaveric spine for signal referencing and to accurately simulate the implant situation. After completion of the MRI scans, the added tissue padding was removed from the cadaveric spine and each implanted intervertebral spacer was imaged by flat-panel detector volume CT.

### **Implants**

In this study, we evaluated 2 metallic intervertebral spacers that differed in shape, material composition, surface properties and implantation method.

The **Intervertebral Body Spacer (IBS)** (Fig. 1a,b) is a titanium aluminum vanadium alloy spacer manufactured by Peter Brehm GmbH, Chirurgie Mechanik, Weisendorf, Germany. This square implant has an evenly ribbed structure on its upper and lower faces and an edge length of 25 x 25 mm. The implant used for this study measured a maximum of 10 mm in height in the anterior segment and had a dorsal inclination of 7°.

The **intervertebral disc dowel (IDD)** (Fig. 2a) is cylindrically shaped spacer made of cobalt chrome molybdenum and manufactured by ESKA Implants GmbH & Co., Luebeck, Germany. Its surface features a 3-dimensional tripodal webbed structure. The IDD used in this study measured 35 mm in length and 15 mm in diameter. The German trade name of this implant is *Bandscheibendübel™*.

## **MRI**

All magnetic resonance imaging studies were conducted on a 1.5T whole-body scanner (Magnetom Symphony, Siemens AG Medical Solutions, Erlangen, Germany). Depending on the sequence, a matrix of 512 x 512 with a field of view (FOV) of 500 mm was selected. T1w-SE and T1w-TSE sequences were used to acquire a slice thickness of 3 mm.

To be able to correlate data records generated by MRI with those obtained by FD-VCT, we intentionally used sequences with short echo times only. Such sequences have markedly lower artifact rates than gradient echo sequences and T2-weighted sequences which both react very sensitively to magnetic fluctuations [3]. Tab. 1 presents the study protocol and lists the target characteristics we focused on in this study.

## **Flat panel detector volume CT (FD-VCT)**

The animal model implanted with the intervertebral spacers was imaged by FD-VCT and the images analyzed (Fig. 3). This prototypical VCT scanner with a flat-panel detector system was developed at the General Electric (GE) Global Research Center (Niskayuna, NY, USA). The system consisted of a Gantry with an x-ray tube [Performix 630, GE Medical Systems, NY, USA] and two flat-panel detectors with arrays of 20.5 x 20.5 cm<sup>2</sup> which perform interlinked rotational movements around a closed rotational center. The x-ray tube has a nominal focus size of 0.7 mm at a peak tube voltage of 140 kV and a tube current of up to 400 mA. The tube power is limited to 20 kW. The weighted computed tomography dose index (CTDI) is 0.172 mGy/mAs measured on a 16 cm Phantom. Since the scanner is not equipped with variable gating of the x-ray beam, it has not yet been approved for clinical application in humans.

The two square flat-panel detectors are arranged at a 120° angle parallel to the system axis. Optionally, the system can be operated using one or two detectors. The two flat-panel detectors consist of a thallium-doped cesium iodide scintillation layer for x-ray absorption and below that a matrix of amorphous silicon diodes. The edge length of each individual detector element is 200 µm. The sensor matrix has a size of 1024 x 1024 pixels, only a portion of which is used for imaging. Parallel to the system axis, both detectors have a continuous readout of 1024 pixels, 180 or 360 lines can be used alternately perpendicular to the system axis. The FD-VCT is operated as an axial system. The gantry aperture has a diameter of 43.8 cm; however the FOV is only 12.8cm x 12.8cm during single-detector operation and 33.3cm x 33.3 cm during dual-detector operation. For the present study, a cuboidal volume range of 42.0 mm edge length was reconstructed from 360 detector lines per rotation, running in single-detector operation.

Thanks to its high detector element density and beam geometry-related radiographic magnification by a factor of 1.43, the FD-VCT permitted the test specimens to be imaged with an isotropic spatial resolution of approx. 140 µm or 3.6 line pairs/mm. The system was also interfaced with several computers for image reconstruction, a data archiving. The images were read and analyzed on an Advantage Windows workstation running Volume Viewer software, Vox volume 3.0.64 [GE Medical Systems, NY, USA].

## **Implantation**

Like the humane spine, the vertebral bodies on the porcine spine increase in size in the craniocaudal direction. The intervertebral spacers were larger than the resected intervertebral discs to account for any implant malalignment and partial expansion in the vertebral canal. The lumbar and thoracic intervertebral disc compartments were dissected to accommodate the intervertebral spacers with central positioning in the transversal plane. The dorsal paravertebral muscles with skin and the ventral sides of the psoas muscles were left attached to the cadaveric spine.

## **Post-imaging processing and analysis**

Following data acquisition were, the image reconstruction was performed by eight parallel running front-end computers [GE Medical Systems]. Data records were further processed on the workstation where adequate colors, contrasts, and opacity were defined for the implanted spacers and algorithms created and applied for examining the specimens. Lastly, multiplanar reconstruction (MPR) and volume-rendering techniques were employed for quantitative determination of length and volume of specific structures.

## **Results**

### **IBS spacer**

**MRI (Fig. 4):** In T1W-TSE sequence, the implant-related artifact boundaries were clearly distinguishable from their surroundings. However, only limited conclusions could be drawn about the extent of fusion between implant and bone because the boundaries between implant and bone were not clearly distinguishable since they were obscured by artifacting, even in the preferred sequences. Although the distinctions that could be made between vertebral canal and implant were satisfactory in general, the overall imaging quality achieved tended to be suboptimal in terms of making an exact assessment of implant position. These MRI studies did not provide conclusive information about current implant shape.

**FD-VCT (Fig. 1 c, d):** FD-VCT produced a practically artifact-free image of the implant situation with excellent detectability of pertinent characteristics such as implant position, implant shape and implant-bone interface. It was also possible to unequivocally evaluate the implant positioning in relation to the vertebral canal. In 3D reconstruction studies, the IBS spacer could be visualized both in its osseointegrated state as well as in isolation. In this regard, FD-VCT permitted determination of the actual implant dimensions, edge length and implant volume. In contrast to MRI, FD-VCT produced sharper-quality image of the implant surface and thereby provided more accurate information about the implant anchorage in relation to the vertebral body and the surrounding structures.

### **Intervertebral disc dowels**

**MRI (Fig. 4):** In T1W-TSE sequence, the implant-related artifact boundaries were as clearly distinguishable from their surroundings as for the titanium IBS spacer. It was not possible to draw conclusions about the extent of the implant-bone contact since the implant-bone boundary was not reproduced, but obscured by artifacts in the preferred sequences. The extreme susceptibility to artifacting that was present only allowed suboptimal distinction between vertebral canal and implant; the imaging quality achieved did not allow conclusive assessment of implant position. Conclusions about the actual implant shape could not be made based on the MRI studies.

**FD-VCT (Fig. 2 b-d):** Similar to the titanium IBS spacer, FD-VCT produced virtually artifact-free images of the implant situation allowing assessment of the target characteristics implant positioning, implant shape and implant-bone interface. Unequivocally assessment of the implant position in relation to the vertebral canal was possible. A 3D reconstruction was additionally prepared that visualized the IBS spacer in its osseointegrated state as well as in isolation. In this context, the current implant dimensions, edge lengths and implant volume could be determined. In contrast to MRI, the FD-VCT produced sharper imaging quality of the implants surface, providing conclusive information about implant anchorage in the adjacent vertebral body.

## **Discussion**

In the diagnostics of pathological processes of the lumbar spine, MRI currently ranks as the standard procedure. Various sequence protocols can be prepared in accordance with the presenting clinical picture. In the clarification of degenerative changes, both T1w and T2w sequence studies are routine practice. However, problems arise when MRI diagnostics are needed when the primary aim is to assess the implant positioning of anterior intervertebral spacers following instrumented lumbar spondylodesis.

In light of the reported disadvantages of auto and allogenic bone grafts [4], the use of interbody cages and spacers made from different materials has become increasing common for bridging the intervertebral disc space in interbody fusions. In this context titanium, carbon fiber-reinforced polymer, cobalt-chrome-molybdenum alloys deserve particular mention. Given the various implant properties relating to the different materials, postoperative MRI diagnostics need to address the following aspects:

1. Assessment of both implant shape and implant positioning
2. Distinction of the implant from the adjacent surroundings

Although the behavior of metallic intervertebral implants in MRI is well documented in the literature [5-11], the individual studies differed greatly with regard to study design and the hypotheses tested. Most studies mainly focused on assessments of sequence-related artifacting and showed that the best imaging quality results for metallic implants were achieved with T1w-SE or T1w-TSE sequences in particular.

The present study investigated intervertebral spacers made of various materials, with the main emphasis being placed on the metallic implants that are difficult to interpret by MRI due to their susceptibility to artifacting. In our experimental setup, this includes the titanium IBS spacer and the cobalt chrome molybdenum alloy intervertebral disc dowel.

In general, the difficulties encountered with the detectability of implants in MRI studies is based on their different magnetizability of various structures resulting from the local magnetic field gradients in the corresponding border regions. In these segments, the spins with different frequencies predominate and lead to signal losses alongside image distortion [12-14]. The larger the difference in susceptibility between bodily tissue and implanted foreign material, the more difficulty the reader has to interpret the image. This problem is of particular importance when it comes to trying to assess implant positioning, implant shape and the implant-bone interface. Depending on the extent of the existing susceptibility to artifacting, reproduction of these characteristics by magnetic resonance imaging is suboptimal. In this connection, satisfactory results can only be achieved with non-metallic implants like the carbon fiber-reinforced polymer spacer we used in this study. Compared to the imaging quality achieved with MRI, FD-VCT [15- 17] allowed an accurate diagnostic interpretation of all target characteristics for all of the implants we tested.

This statement specifically applied to the visualization of the implant-bone interface, which even in plain radiographs can only be assessed to a limited extent. In addition to the reliable detection of implant positioning, additionally implant-related findings were obtained that were not obtainable by MRI diagnostics. Here, the sharp reproduction of implant shape and existing implant surface structures deserves special mention. The optional 3D reconstruction provided further, implant-specific data such as length and volume.

With FD-VCT, the intervertebral spacers could be clearly distinguished from their surroundings regardless of the material used. Thus, FD-VCT appears to be the ideal modality in preclinical studies for evaluation of osseous integration processes secondary to interbody spondylodesis. The studies to be conducted in this regard might focus on the use of bone substitutes and specially coated implants. Moreover, it would be interesting to image the potential changes would spinal models undergo during load-bearing tests. The current prototype lacks a variable gating of the x-ray beam and is therefore only suited for experimental applications. A clinical application might be conceivable after the appropriate technical modifications to the FD-VCT prototype. The superior imaging quality of the implant situation, particular of metallic intervertebral spacers in situ might lead to more optimal postoperative diagnosis of potentially implant-related complications secondary to interbody fusions interventions.

## **References**

- Cizek GR, Boyd LM (2000) Imaging pitfalls of interbody spinal implants. *Spine* 25: 2633-2636.
- Kiessling F, Greschus S, Lichy MP et al. (2004) Volumetric computed tomography (VCT): A new technology for noninvasive, high-resolution monitoring of tumor angiogenesis. *Nat Med* 10: 1133-1138.
- Herold T, Caro WC, Heers G et al. (2004) Abhängigkeit der Artefaktgröße vom Sequenztyp in der MRT-Präparatstudie zur Beurteilung der postoperativen Schulter nach Labrumfixation. *Fortschr Röntgenstr* 176: 1296-1301.
- Goulet JA, Senunas LE, DeSilva GL et al. (1997) Autogenous iliac crestbone graft. Complications and assessment. *Clin Orthop* 339: 76-81
- Henk CB, Brodner W, Grampp S et al. (1999) The postoperative spine *Top Magn Reson Imaging* 10: 247-264
- Malik AS, Boyko O, Atkar N et al. (2001) A comparative study of MR imaging profile of titanium pedicle screws. *Acta Radiol* 42: 291-293.
- Ortiz O, Pait TG, McAllister P et al. (1996) Postoperative magnetic resonance imaging with titanium implants of the thoracic and lumbar spine. *Neurosurgery* 38: 741-745.
- Petersilge CA, Lewin JS, Duerk JL et al. (1996) Optimizing imaging parameters for MR evaluation of the spine with titanium pedicle screws. *Am J Roentgenol* 166: 1213-1218.
- Rupp R, Ebraheim NA, Savolaine ER et al. (1993) Magnetic resonance imaging evaluation of the spine with metal implants. General safety and superior imaging with titanium. *Spine* 18: 379-385.
- Wang JC, Yu WD, Sandhu HS et al. (1998) A comparison of magnetic resonance and computed tomographic image quality after the implantation of tantalum and titanium spinal instrumentation. *Spine* 23: 1684-1688.
- Wang JC, Sandhu HS, Yu MD et al. (1997) MR parameter for imaging titanium spinal instrumentation. *J Spinal Disord* 10: 27-32.
- Fellner C, Behr M, Fellner F et al. (1997) Artifacts in MR imaging of the temporomandibular joint caused by dental alloys: a phantom model study at T1.5. *Fortschr Röntgenstr* 166: 421-428.

Fritzsche S, Thull R, Haase A (1994) Reduction of artifacts in magnetic resonance images by using optimized materials for diagnostic devices and implants. Biomed Tech (Berl) 39: 42-46.

Schenck JF (1996) The role of magnetic susceptibility in magnetic resonance imaging: MRI magnetic compatibility of the first and second kinds. Med Phys 23: 815-850.

Kalender WA (2003) Der Einsatz von Flachbilddetektoren für die CT-Bildgebung. Radiologie 43: 379-387.

Ning R, Chen B, Yu R et al. (2000) Flat panel detector-based-cone-beam volume CT angiography imaging: system evaluation. IEEE Trans Med Imaging 19: 949-963.

Ning R, Tang X, Conover D et al. (2003) Flat panel detector-based cone beam computed tomography with a circle-plus-two-arcs data acquisition orbit: preliminary phantom study. Med Phys 30: 1694-1705.

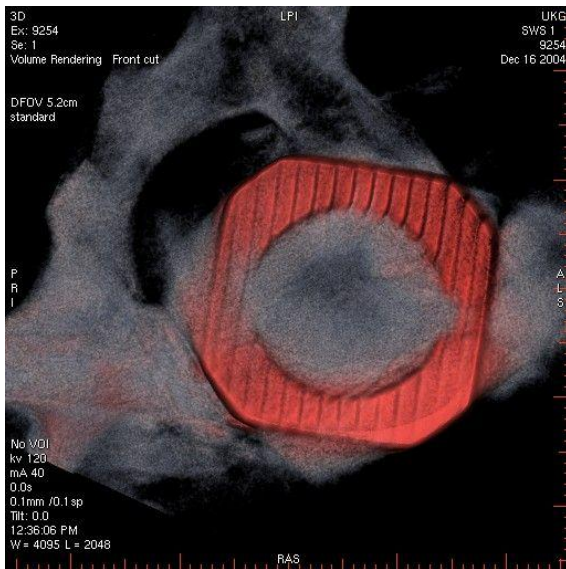
**Figure Legends**

Fig. 1: Titanium intervertebral body spacer (IBS): a, b: Cranial and lateral view of the original implant, c, d: FD-VCT: 3D implant imaging with artifact-free visualization of implant position

**Figure 1a**



**Figure 1b**



**Figure 1c**

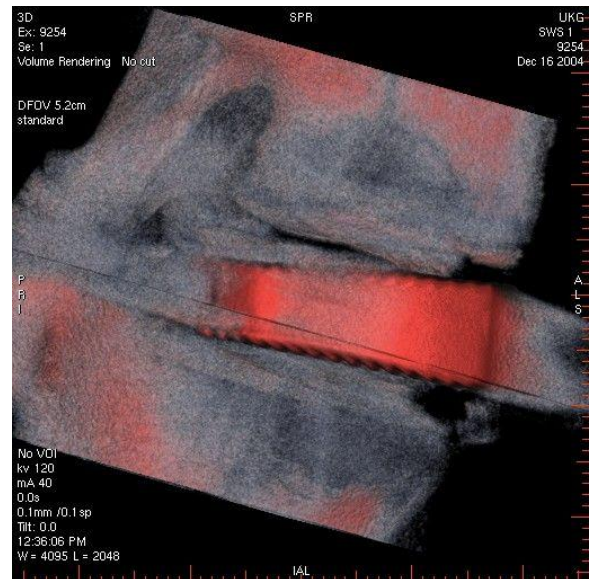


**Figure 1d**

Fig. 2: Intervertebral disc dowel (CoCrMo): a: Original implant, b, c: FD-VCT: 3D implant imaging including volumetry, d: FD-VCT: Sagittal plane with artifact-free visualization of implant shape and position

Figure 2a



Figure 2b

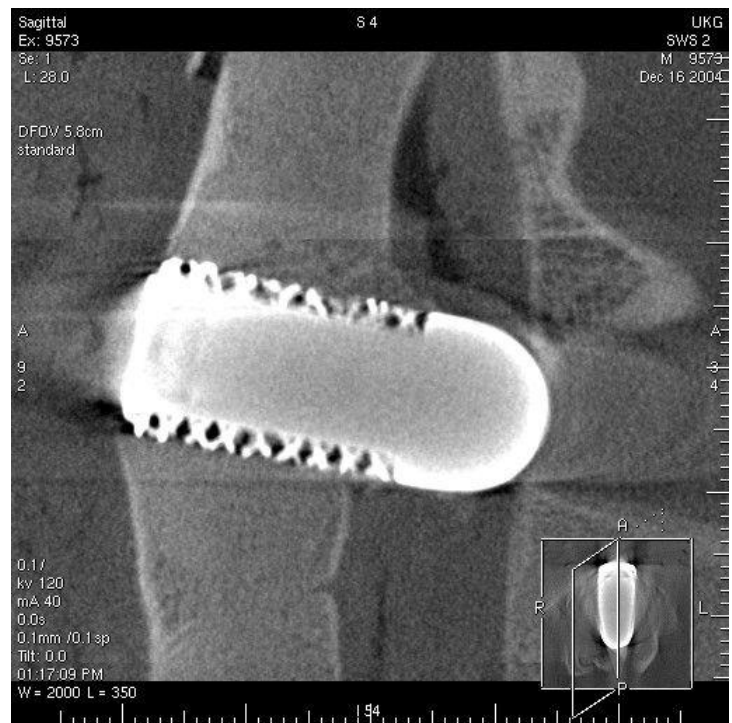
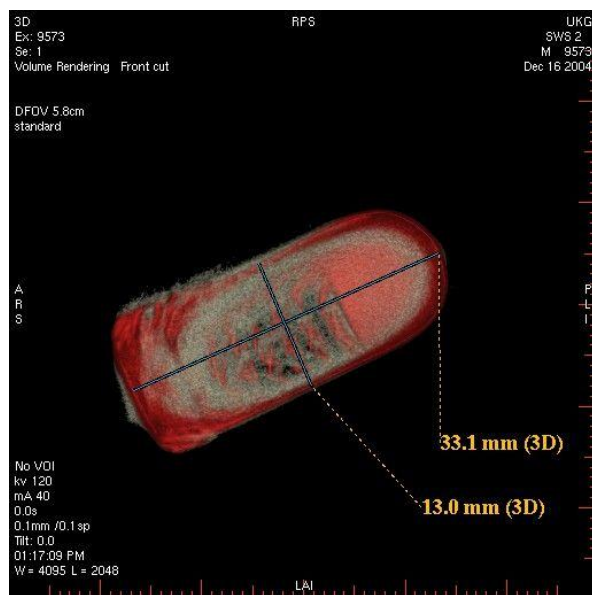
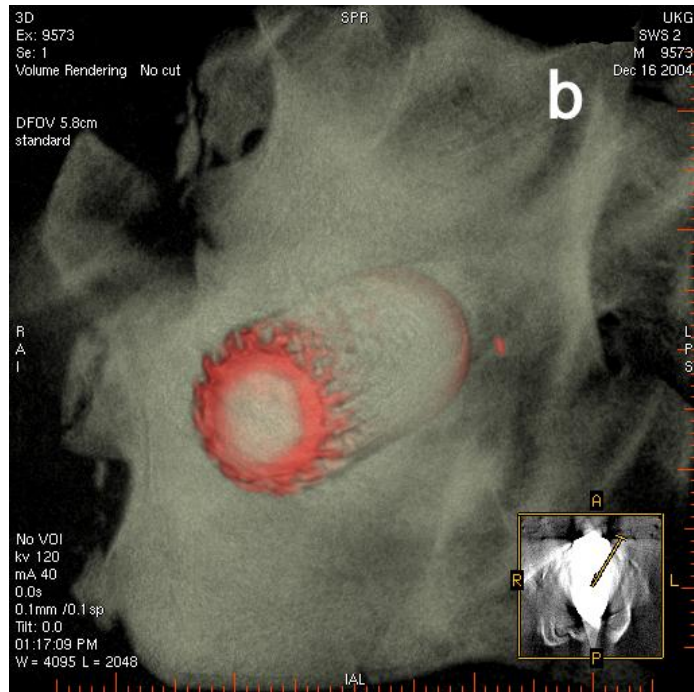


Figure 2c

Figure 2d

Fig. 3: Flat-panel detector-based volume computed tomograph (GE Global Research Center, Niskayuna, N.Y.)



Fig. 4: MRI of the experimental implants: a: CoCrMo intervertebral disc dowel, b: Titanium IBS spacer.

